Paper III

Thermal stability and biochemical properties of isocitrate dehydrogenase from the thermoacidophilic archaeon *Thermoplasma acidophilum*

Runar Stokke, Nils-Kåre Birkeland and Ida H. Steen*

Department of Biology, University of Bergen, P.O. Box 7800 Jahnebakken 5, 5020 Bergen, Norway

Abbreviations: *IDH* isocitrate dehydrogenase - *TaIDH Thermoplasma acidophilum* IDH - *AfIDH Archaeoglobus fulgidus* IDH - *PfIDH Pyrococcus furiosus* IDH - *EcIDH Escherichia coli* IDH - *SDS-PAGE* Sodium dodecyl sulfate-polyacrylamide gel electrophoresis - *DSC* differential scanning calorimetry - T_m melting temperature.

*Corresponding author: Ida Helene Steen Tel: +47 - 55 58 83 75; Fax +47 – 55589671
Email: Ida.Steen@bio.uib.no

Abstract

Isocitrate dehydrogenase [IDH; EC 1.1.1.42] from the thermoacidophilic archaeon *Thermoplasma acidophilum* (*Ta*IDH) showed high thermal stability with an apparent melting temperature, T_m, of 82.2 °C and 84.5 °C at pH 7.5 and 5.8, respectively. Based on structural alignment of *Ta*IDH with IDH from *Aeropyrum pernix* (*Ap*IDH) and *Archaeoglobus fulgidus* (*Af*IDH) residues forming an aromatic cluster in the clasp-domain thought to strengthen the dimer interface in *Ap*IDH and *Af*IDH were identified in the former enzyme. Moreover, *Ta*IDH had a shortened N-terminus that may protect the enzyme from thermal denaturation. The enzyme activity of *Ta*IDH was highest at 70 °C. The pH-activity profile was bell-shaped with an optimum shifted to a lower pH compared to *Af*IDH. The activity of *Ta*IDH was influenced on changes in pH with a three-fold reduction in activity when the pH was shifted from the pH-optimum at 7.5 to pH 5.8. However, the specific activity at pH 5.8 was still high when compared with *Af*IDH. The reduction in activity at pH 5.8 was not due to instability of the enzyme as the T_m of *Ta*IDH was higher at pH 5.8 than at 7.5 and the enzyme retained 91 % of its activity after incubation at one hour at pH 5 and 60 °C. The differences in the pH activity profiles of *Ta*IDH in comparison with *Af*IDH may thus be related to the pK_as of their catalytic residues involved in the initial proton abstraction and the final proton donation during the catalysis of oxidative decarboxylation of isocitrate to 2-oxoglutarate and reduced coenzyme.

Keywords: Isocitrate dehydrogenase; *Thermoplasma acidophilum*; thermal stability; thermoactivity; acidophilic.

Isocitrate dehydrogenase (IDH) belongs to the metal-dependent (Mg^{2+} or Mn^{2+}) β-decarboxylating dehydrogenases, an enzyme in the tricaboxylic acid cycle which catalyses the oxidative decarboxylation and subsequent dehydrogenation of D-isocitrate to α-ketoglutarate and CO_2 using NAD^+ (EC 1.1.1.41) or $NADP^+$ (EC 1.1.1.42) as cofactor (Hurley et al. 1991). IDHs are broadly distributed throughout Bacteria, Eukarya and Archaea (Steen et al. 2001) and based on primary sequence identity, IDHs have previously been divided into three distinct phylogenetic subfamilies, subfamily I (NAD(P)-IDHs from archaea and bacteria), subfamily II (NADP-IDHs from eukarya and bacteria) and subfamily III (NAD-IDHs from eukarya) (Steen et al. 2001). The crystal structures of $NADP^+$-dependent IDH from *Escherichia coli* (Hurley et al. 1989) (*Ec*IDH), *Bacillus subtilis* IDH (Singh et al. 2001) (*Bs*IDH), *Archeaoglobus fulgidus* (Stokke et al. submitted to FEBS Journal 2006) (*Af*IDH) and *Aeropyrum pernix* (Karlström et al. 2005) (*Ap*IDH) have revealed a high structural similarity between intra-family members of subfamily I. However, the thermal properties among these IDHs vary significantly with *Ap*IDH and *Af*IDH being most thermostable with apparent melting temperatures, T_ms, of 109.9 and 98.5 °C, respectively, in comparison with the T_m of 52.6 °C of *Ec*IDH. Structural comparisons of *Ap*IDH and *Af*IDH with *Ec*IDH have revealed fixation of the N-terminus, shortening of surface loops, inter-domain ionic networks and aromatic clusters for stabilising the dimer interface as putative major mechanisms for increasing the thermal stability of the two former enzymes (Karlström et al. 2005)(Stokke et al. submitted to FEBS Journal 2006)

Data regarding the thermal properties of IDH from *Thermoplasma acidophilum* (*Ta*IDH) will provides valuable information in the mid-range temperature area in between the IDHs from the hyperthermophilic *A. pernix* and *A. fulgidus* and the IDH from the mesophilic *E. coli*.

Wild-type *T. acidophilum* DSMZ 1728 cells were cultivated aerobically at 59 °C in medium 158 as described in DSMZ. Genomic DNA was isolated using AquaPure Genomic DNA Isolation Kit from BioRad (Bio-Rad Laboratories Ltd., United Kingdom) according to the manufacturer instructions. The putative *idh* gene from *T. acidophilum,* as amplified by PCR using the following primer sets;

5`- CACCATGGCATATATTCAAGTGAAGGAGG-3` and 5`-AAGCCTTTAGTGAACAGGTTTTTTCATCCTGTTG-3`, was found to contain a high percentage of *E. coli* rare codons, AGG and AGA coding for arginine. Hence, expression of *Ta*IDH in *E. coli* BL21 was performed in the presence of a plasmid (pSJS1240) which expressed the argU and ileX genes encoding rare tRNAs (Kim et al. 1998). 12 of the total 17 arginines in *Ta*IDH were encoded by AGG, whereas none of the total 17 arginines were encoded by AGG in *Ec*IDH. The over-expression of recombinant *Ta*IDH in *E. coli* strain BL21/pSJS1240 was performed by growing transformed cells in LB broth containing ampicillin (100 μg/ml) and spectinomycin (50 µg/ml) at 37 ºC to OD_{600} = 0.7-0.8 and subsequent expression (3-4 h) after addition of 1.0 mM isopropyl-beta-D-thiogalactopyranoside. The purification of recombinant *Ta*IDH was performed as previously described for other archaeal IDHs (Steen et al. 2001) and resulted in a high yield of purified enzyme (Table 1). However, the amount of purified recombinant *Ta*IDH of 3 mg pure protein/liter culture was considerable lower than previously obtained for other archaeal IDHs (Steen et al. 2001). This result indicates a low expression level of *Ta*IDH in *E. coli* despite the presence of the plasmid pSJS1240. The enzyme was purified to homogeneity as assessed by sodium dodecyl sulfate-polyacrylamide gel electrophoresis (SDS-PAGE) with Coomassie blue staining.

All amino acid residues involved in binding of isocitrate in *Ec*IDH and *Ap*IDH from subfamily I were conserved in *Ta*IDH (Fig. 1). Purified recombinant *Ta*IDH showed no activity when NAD^+ was used as cofactor in concentration up to 2 mM, but showed preference for $NADP^+$ with a K_m of 111 µM. This result is supported by the conservation (Fig. 1) of amino acids involved in cofactor specificity in the $NADP^+$-dependent *Ec*IDH (Hurley et al. 1991; Dean and Golding 1997). This result contradicts the data reported on enzyme activity measurements in crude exstract from *T. acidophilum* indicating *Ta*IDH as having dual-cofactor spesificity (Potter 1993).

*Ta*IDH had highest specific activity at 70 °C (Fig.2a), i.e, 11 °C higher then the growth optimum of the host organism (Table 2). At 70 °C *Ta*IDH showed a half-life ($t_{1/2}$) of 88 min which decreased to 24 min when the temperature was increased to 75 °C (Fig.2b). The thermal stability of *Ta*IDH was furthermore estimated by differential scanning calorimetry (DSC). As previously found for IDHs (Steen et al. 2001), the thermal unfolding of *Ta*IDH was found to be an irreversible process. Hence, only an apparent midpoint T_m could be determined. At pH 7.5 a T_m of 82.2 °C was found for *Ta*IDH and the value shows that *Ta*IDH has a thermal stability midway between *Ap*IDH and *Af*IDH respectively, and *Ec*IDH (Table 2). Interestingly, at pH 5.8, close to the reported intracellular pH of the host organism (Searcy 1976), *Ta*IDH revealed a T_m of 84.6 °C, i.e, 2.3 °C higher than at pH 7.5 (Fig.2c). The acid tolerance of *Ta*IDH, compared to *Af*IDH, was further estimated by incubating the enzymes for one hour at pH 3, 4 and 5 and measuring the residual activity. *Ta*IDH was found to be moderate acid tolerant with 81 % residual activity remaining after 1 hour at pH 4.0. In comparison, *Af*IDH showed only 67 % residual activity. Both enzymes were inactive after 1h at pH 3.0 (not shown).

Structure analysis of homodimeric *Ap*IDH and *Af*IDH revealed a conserved aromatic cluster in the clasp-domain formed by three aromatic residues from each monomer (Karlström et al. 2005) and *Af*IDH (Stokke et al. submitted to FEBS Journal 2006). This aromatic cluster is thought to strengthen the subunit interactions and contribute to the high thermal stability observed for these enzymes. An aromatic cluster may also be formed in *Ta*IDH as the residues involved are conserved in its primary structure; Trp154, Phe167 and Phe172 (Fig. 1). The residues involved in a 4-membered ionic network from the clasp-domain of one subunit to the small domain of the adjacent subunt in *Af*IDH were however not conserved in the sequence of *Ta*IDH. However, the loop shortening observed in the clasp-domain of *Af*IDH compared to *Ec*IDH was also observed in the sequence of *Ta*IDH, i.e, further stabilising *Ta*IDH compared to *Ec*IDH. One of the strategies of the hyperthermostable IDHs to maintain the integrity of the structure at high temperature has been

protection of the N-terminus. In *Ap*IDH, a disulfide in the N-terminus was confirmed by mutagenesis to be involved in the stability above 100 °C, as disruption of the disulfide reduced the T_m from 109.9 °C to 100.3 °C (Karlström et al. 2005). In the structure of *Af*IDH, no disulfide was observed. However, the N-terminus of *Af*IDH was shown to be shorter than in *Ap*IDH. Furthermore, an aromatic cluster in the N-terminus of *Af*IDH was suggested to stabilize this region. The N-terminus of *Ta*IDH was shown to be shorter than both the mesostable *Ec*IDH and the hyperthermostable *Pf*IDH, *Af*IDH and *Ap*IDH with 9, 7, 10 and 18 amino acids, respectively (Fig. 1). Hence, a substantial shortening in this area could protect the N-terminus and aid in the protection of *Ta*IDH from thermal degradation. Previous studies on citrate synthase (CS) have shown no interactions in the N-terminus of *Ta*CS to be essential for its thermal stability (Bell et al. 2002). In *Ap*IDH, a seven-membered network was located between the large and the small domain at the opposite side of the active site (Karlström et al. 2005). Analysis of *Af*IDH found three of these residues conserved in an ionic network. Sequence comparisons revealed the same three residues conserved in the *Ta*IDH sequence (Asp112, Arg194 and Asp315). However, the three residues were also conserved in *Ec*IDH. A structure of *Ta*IDH is being pursued in order to investigate the molecular elements involved in the thermal stability of this enzyme.

Thermoacidophiles are highly adapted to the high temperature and the harsh environment of low pH (0-4) by maintaining a intracellular pH close to neutral (Darland et al. 1970; Searcy 1976; van de Vossenberg et al. 1998; Macalady et al. 2004). Activity measurements of *Ta*IDH at various pH values revealed a bell shaped pH-activity profile (Fig. 2d) with an optimum shifted to a lower pH compared with *Af*IDH. At 60 °C *Ta*IDH showed the highest activity at pH 7.5. However, the activity in 20 mM sodium-phosphate revealed large differences between pH 7.3-7.5. In comparison, the pH-optimum for activity of *Af*IDH has previously been found to be pH 8.6 (Steen et al. 1997). Furthermore, the pH profile of *Ta*IDH and *Af*IDH revealed the activity of *Ta*IDH as highly buffer- and pH-dependent compared to *Af*IDH (Fig. 2d). At pH 5.6, close to the physiological intracellular

pH of *T. acidophilum* at pH 5.5 (Searcy 1976), *Ta*IDH still sustained a high specific activity as compared to *Af*IDH. The pH optimum of activity for *Ta*IDH is approximately 2 pH units above the intracellular pH of the host organism (Searcy 1976). Similar observations have also been found for glucose dehydrogenase (GDH) from *P. torridus* (Angelov et al. 2005). The decreased activity at pH 5.6 compared to pH 7.5 is not ascribed to an inactivation of *Ta*IDH since incubation at pH 5 and 60ºC retained approx 91 % initial activity of the enzyme. The bell shaped pH-activity profile of *Ta*IDH could be explained by the ionization states of two catalytic residues involved in the conversion of isocitrate to α-ketoglutarate. The oxidative decarboxylation of isocitrate to α-ketoglutarate and NADPH proceeds in two steps. In the initial step, isocitrate is oxidized to oxalosuccinate by the removal of a proton from the hydroxyl oxygen to a base and the transfer of a hydride to $NADP^+$. In *Ec*IDH, the base was suggested to be Asp283 (Hurley et al. 1991). However, in porcine IDH and *Ap*IDH a active-site water molecule was suggested to accept this proton as part of a proton relay to the solvent (Ceccarelli et al. 2002; Karlström et al. 2005). Second, the β-carboxylate of oxalosuccinate is lost as CO_2 followed by the stereospecific protonation of the β-carbon to form α-ketoglutarate. In *Ec*IDH, Tyr160 and Lys230´ was shown to be hydrogen-bonded to the β-carboxylate of isocitrate and acted as acid catalyst that protonated C3 after decarboxylation (Hurley et al. 1991). The observed shift in pH-optimum in *Ta*IDH compared to *Af*IDH could be a result of a pKa change of the two catalytic residues Asp283 and Lys230 (*Ec*IDH numbering). This was, however, not as extreme as for extracellular acidophilic enzymes, but rather in agreement with previously observed characteristics for intracellular enzymes from acidophilic organisms (Richter and Schafer 1992; Nemoto et al. 2003; Hansen et al. 2004; Angelov et al. 2005)

Acknowledgements

This work was supported by the Norwegian Research Council (Project no. 153774/420). We are grateful to Dr. Aurora Martinez, Department of Biomedicine, University of Bergen, for access to her laboratory facilities and expertise in use of differential scanning calorimetry. The excellent laboratory skills of Lisbeth Glærum and Marit Steine Madsen are also much appreciated.

References

Angelov, A., Futterer, O., Valerius, O., Braus, G.H., and Liebl, W. 2005. Properties of the recombinant glucose/galactose dehydrogenase from the extreme thermoacidophile, *Picrophilus torridus*. *FEBS Journal* **272:** 1054-1062.

Bell, G.S., Russell, R.J.M., Connaris, H., Hough, D.W., Danson, M.J., and Taylor, G.L. 2002. Stepwise adaptations of citrate synthase to survival at life's extremes. From psychrophile to hyperthermophile. *Eur J Biochem* **269:** 6250-6260.

Ceccarelli, C., Grodsky, N.B., Ariyaratne, N., Colman, R.F., and Bahnson, B.J. 2002. Crystal structure of Porcine mitochondrial $NADP^+$-dependent isocitrate dehydrogenase complexed with Mn^{2+} and isocitrate. Insights into the enzyme mechanism. *J Biol Chem* **277:** 43454-43462.

Darland, G., Brock, T., Samsonoff, W., and Conti, S. 1970. A thermophilic, acidophilic mycoplasma isolated from a coal refuse pile. *Science* **170:** 1416-1418.

Dean, A.M., and Golding, G.B. 1997. Protein engineering reveals ancient adaptive replacements in isocitrate dehydrogenase. *PNAS* **94:** 3104-3109.

Gouet, P., Courcelle, E., Stuart, D., and Metoz, F. 1999. ESPript: analysis of multiple sequence alignments in postscript. *Bioinformatics* **15:** 305-308.

Hansen, T., Wendorff, D., and Schonheit, P. 2004. Bifunctional phosphoglucose/phosphomannose isomerases from the archaea *Aeropyrum pernix* and T*hermoplasma acidophilum* constitute a novel enzyme family within the phosphoglucose isomerase superfamily. *J. Biol. Chem.* **279:** 2262-2272.

Hurley, J.H., Dean, A.M., Koshland, D.E., and Stroud, R.M. 1991. Catalytic mechanism of $NADP^+$-dependent isocitrate dehydrogenase - Implications from the structures of magnesium isocitrate and $NADP^+$ complexes. *Biochemistry* **30:** 8671-8678.

Hurley, J.H., Thorsness, P.E., Ramalingam, V., Helmers, N.H., Koshland, D.E.J., and Stroud, R.M. 1989. Structure of a bacterial enzyme regulated by phosphorylation, isocitrate dehydrogenase. *Proc Natl Acad Sci U S A* **86:** 8635-8639.

Karlström, M., Stokke, R., Steen, I.H., Birkeland, N.-K., and Ladenstein, R. 2005. Isocitrate dehydrogenase from the hyperthermophile *Aeropyrum pernix*: X-ray structure analysis of a ternary enzyme-substrate complex and thermal stability. *J Mol Biol* **345:** 559-577.

Kim, R., Sandler, S.J., Goldman, S., Yokota, H., Clark, A.J., and Kim, S.-H. 1998. Overexpression of archaeal proteins in *Escherichia coli*. *Biotechnology Letters* **20:** 207-210.

Macalady, J.L., Vestling, M.M., Baumler, D., Boekelheide, N., Kaspar, C.W., and Banfield, J.F. 2004. Tetraether-linked membrane monolayers in *Ferroplasma* spp: a key to survival in acid. *Extremophiles* **8:** 411-419.

Nemoto, N., Oshima, T., and Yamagishi, A. 2003. Purification and characterization of geranylgeranylglyceryl phosphate synthase from a thermoacidophilic archaeon, *Thermoplasma acidophilum*. *J Biochem (Tokyo)* **133:** 651-657.

Potter, S. 1993. Evidence for a dual-specificity isocitrate dehydrogenase in the euryarchaeotan *Thermoplasma acidophilum*. *Canadian Journal of Microbiology* **39:** 262-264.

Richter, O.-M.H., and Schafer, G. 1992. Purification and enzymic characterization of the cytoplasmic pyrophosphatase from the thermoacidophilic archaebacterium *Thermoplasma acidophilum*. *Eur J Biochem* **209:** 343-349.

Searcy, D.G. 1976. *Thermoplasma acidophilum*: Intracellular pH and potassium concentration. *Biochimica et Biophysica Acta (BBA) - General Subjects* **451:** 278-286.

Singh, S.K., Matsuno, K., LaPorte, D.C., and Banaszak, L.J. 2001. Crystal structure of *Bacillus subtilis* isocitrate dehydrogenase at 1.55 Å. Insights into the nature of substrate specificity

exhibited by *Escherichia coli* isocitrate dehydrogenase kinase/phosphatase. *J Biol Chem* **276:** 26154-26163.

Steen, I.H., Lien, T., and Birkeland, N.K. 1997. Biochemical and phylogenetic characterization of isocitrate dehydrogenase from a hyperthermophilic archaeon, *Archaeoglobus fulgidus*. *Arch Microbiol* **168:** 412-420.

Steen, I.H., Madern, D., Karlstrom, M., Lien, T., Ladenstein, R., and Birkeland, N.-K. 2001. Comparison of isocitrate dehydrogenase from three hyperthermophiles reveals differences in thermostability, cofactor specificity, oligomeric state, and phylogenetic affiliation. *J Biol Chem* **276:** 43924-43931.

van de Vossenberg, J.L.C.M., Driessen, A.J.M., Zillig, W., and Konings, W.N. 1998. Bioenergetics and cytoplasmic membrane stability of the extremely acidophilic, thermophilic archaeon *Picrophilus oshimae*. *Extremophiles* **2:** 67-74.

Tables

Table 1. Purification of recombinant *Ta*IDH expressed in *E. coli* BL21 (pSJS1240).

	Total protein/liter culture (mg)	Total activity (U)	Specific activity (U/mg)	Yield (%)
Crude extract	187.3	1836	27	100
Heat treatment (60 °C)	140	1821.25	23.5	99.2
Red Sepharose affinity chromatograpy	3	1190	396.7	64.8

Table 2. Thermal properties of IDH from mesophilic and (hyper)thermophilic microorganisms.

Organisms	T_{growth} (°C)	T_{opt} (°C)	T_m (°C)
P. furiosus	100	≥95	103.7*
A. pernix	90-95	≥95	109.9*
A. fulgidus	83	90	98.5*
T. acidophilum	59	70	82.2
E. coli	37	50	52.6**

T_{growth}: optimal temperature for growth of the organism. T_{opt}: temperature at which optimal enzymatic activity occurs. T_m: melting temperature as determined by differential scanning microcalorimetry in 50 mM potassium phosphate pH 7.5, 0.1 M NaCl

* (Steen et al. 2001)

** (Karlström et al. 2005)

Legends to figures

Figure 1. Sequence alignment of IDH sequences from archaea; *Af*IDH (CAB09535), *Ta*IDH (NP_393595), *Aeropyrum pernix* IDH (*Ap*IDH; NP_147421) and *Pyrococcus furiosus* IDH (*Pf*IDH; NP_577931), and bacterial IDH from *Escherichia coli* (*Ec*IDH; NP_415654). The sequence alignment was made in clustalW and secondary structure assignments were added in ESPript (Gouet et al. 1999). Secondary structure assignments was given the nomenclature as implemented in *Ec*IDH (Hurley et al. 1989), *Ap*IDH (Karlström et al. 2005) and *Af*IDH (Stokke et al. submitted to Extremophiles 2006) Amino acids responsible for binding of isocitrate and the discrimination of cofactor $NADP^+$ in *Ec*IDH are marked with boxes and stars, respectively.

Figure 2. a Temperature optimum for activity of *Ta*IDH as determined spectrophotometrically by monitoring the conversion of $NADP^+$ to NADPH at 340 nm and varying temperatures from 35 – 80 °C in 50 mM Tricine/KOH pH 7.0. **b** Inactivation of *Ta*IDH in a glycerol bath at given temperatures; 60 (●), 65 (○), 70 (▼) and 75 °C (▽). Aliquots were removed at given time intervals, 0 – 120 min, snap-cooled on ice and residual activity was determined at 60 °C in 50 mM Tricine/KOH pH 7.5. **c** Apparent melting temperatures, T_m, as determined by differential scanning calorimetry (DSC) in 50 mM potassium-phosphate, 0.1 M NaCl, pH 5.8 and 7.5. The calorimetric scans were carried out between 20 and 100 °C with a scan rate of 1 K/min. A second scan was run to estimate reversibility. Apparent T_ms were determined from the transition midpoint upon unfolding, due to the irreversible nature of the enzyme. **d** pH-profile for activity of *Ta*IDH with *Af*IDH as control. The profiles were determined with two buffer systems; 20 mM sodium-phosphate pH 5.6 – 8.0 (● *Ta*IDH and ▲ *Af*IDH) and 50 mM Tricine/KOH pH 7.0 – 8.5 (■ *Ta*IDH and ◘ *Af*IDH).

Figures

Fig.1

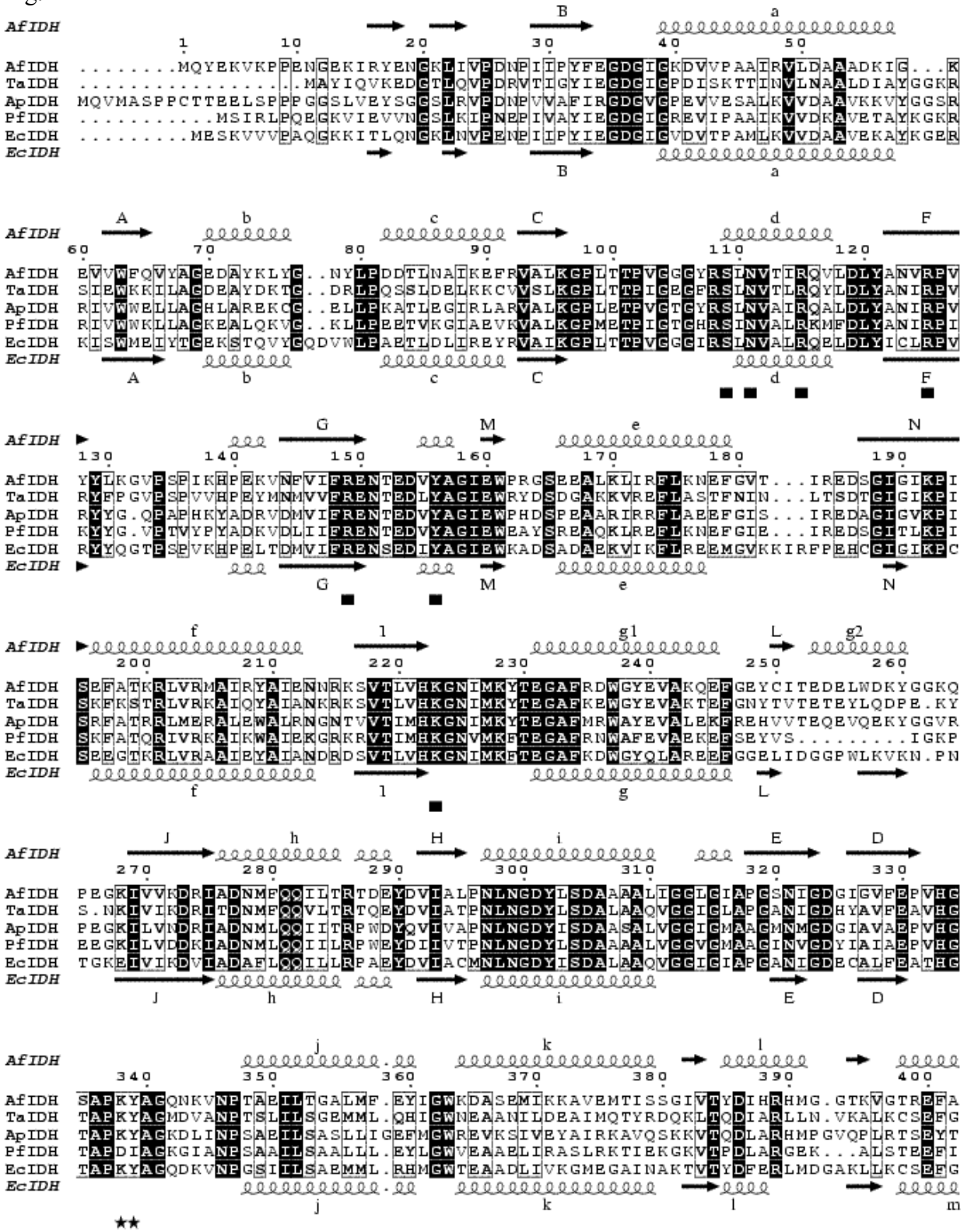

Fig. 2

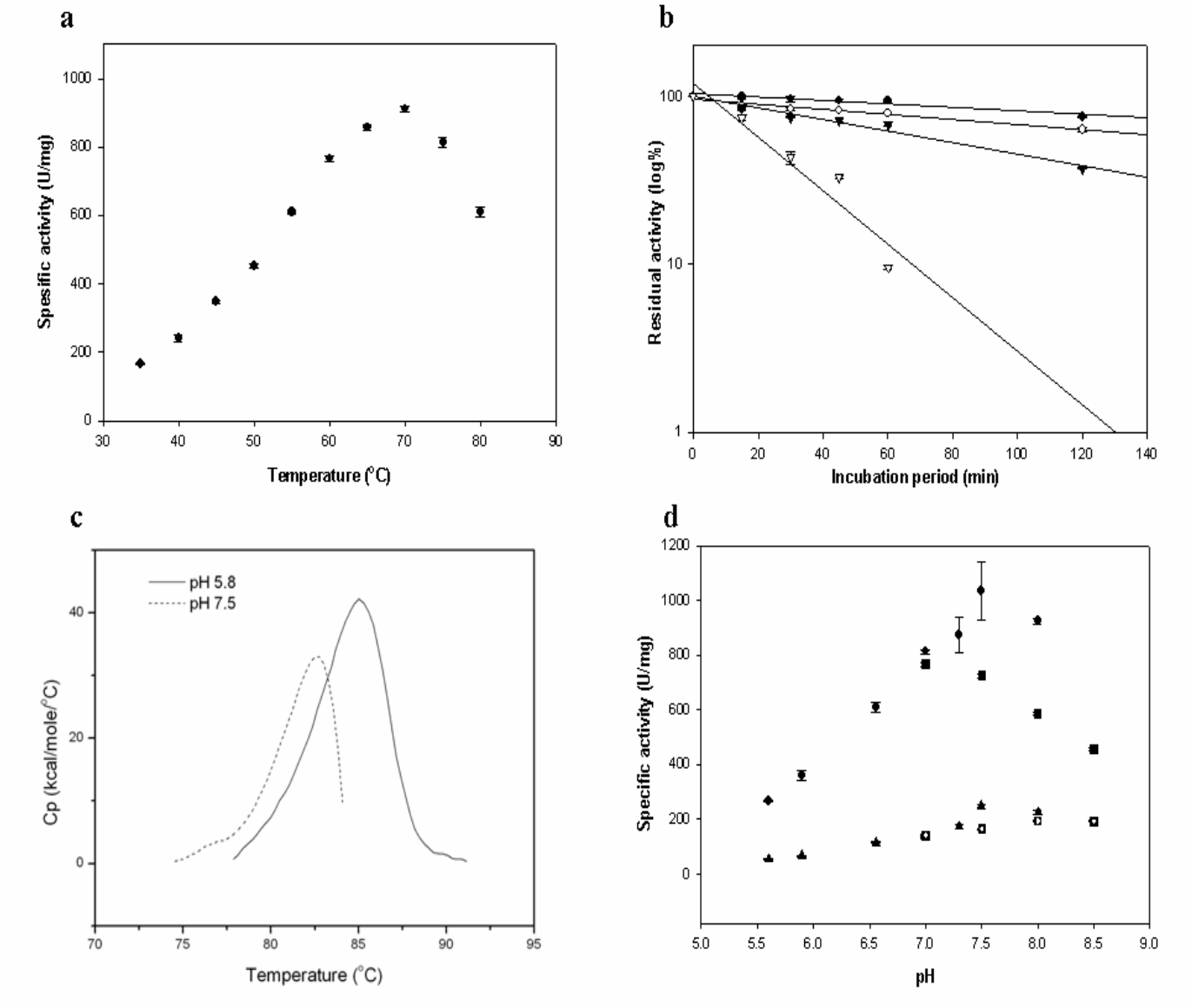
a
Spesific activity (U/mg)
Temperature (°C)
b
Residual activity (log%)
Incubation period (min)
c
pH 5.8
pH 7.5
Cp (kcal/mole/°C)
Temperature (°C)
d
Specific activity (U/mg)
pH